



ANALYSIS OF A SQUAT CONCRETE WALL, DIFFERENCE IN TRANSLATION DURING SEISMIC EXCITATION DUE TO FOUNDATION SUPPORT.

E. R. Thorhallsson¹, I. S. Rikhardsson², A.M. Olafsson³ and H.S. Olafsson⁴

ABSTRACT

In this study a squat concrete wall is examined, and how different foundation support changes the wall's behavior during seismic excitation. A case is examined where the wall is rigidly fixed to the ground and the results are compared with a scenario where the foundation is allowed to rock and undergo translation on a thin 0.5 m gravel isolation layer. The wall and support were modeled using finite element method (FEM). The FEM calculations were carried out using the program ANSYS. The soil-structure interaction (SSI) model was separated into near-field and far-field using FEM to represent the near-field and viscous dampeners placed around the FEM model as boundary elements to represent the far-field. The results show that the difference in motion and energy dissipation is significant between a normally fixed base scenario versus the case where rocking and translation is allowed; the motion increases while stress decreases and the energy dissipation is due to the friction and pounding between the foundation and the support.

Introduction

In the field of structural engineering it is common while carrying out a structural design to assume the foundation to be fixed to the ground. This is done to simplify calculations and to deliver quick solutions for static load cases and design combinations. Earthquake structural codes also adopt this approach and anticipate that energy dissipation in shear walls, made to resist earthquake forces, occurs at the base of the wall due to plastic deformation in its longitudinal reinforcement. During earthquakes fixed-ground approach does not accurately depict the dynamic behavior of the structure. Since the supporting medium can deform, the overall stiffness of the system is overestimated when using fixed approach (Dutta 2004). Also due to sliding and rocking the displacements in shear walls are greater than calculated. This has led to failures in frame systems with shear walls made to resist earthquake forces, where the displacements of the wall have caused greater P-delta effects on connected adjacent support columns. However stress distribution has shown to be favorable in these cases (Apostolou 2007, Zang 2009). It can be assumed that the greater the lateral loads on the shear wall the less sliding and rocking will occur.

This approach of calculating the behavior of the shear wall during earthquakes shows larger displacements while decreasing the average stress throughout the wall, and the energy dissipation will be mainly due to its rocking and translation. Soil-structure interaction (SSI) is also examined.

¹Associate Professor, Dept. of Civil Engineering, Reykjavik University, Iceland

²Assistant Professor, Dept. of Mechanical Engineering, Reykjavik University, Iceland

³Graduate Research Assistant, Dept. of Civil Engineering, Reykjavik University, Iceland

⁴Graduate Research Assistant, Dept. of Civil Engineering, Reykjavik University, Iceland

For SSI problems it's most practical to divide the model into near-field and far-field. The near-field includes the structure and the support it rests on and its numerical solution obtained either with:

1. Domain type methods, for example Finite Element Method (FEM) or
2. Boundary type methods, such as Boundary Element Method (BEM).

Domain type method is used to represent the near-field in this study; this method leads to reaction of waves at the truncated boundaries back to the domain of the model. The far-field represents the infinity of the soil. Many approaches have been suggested to do so, FEM cloning, infinite elements and BEM methods. It was decided to use the BEM to simulate the infinity as viscous dampers around the near-field truncated boundaries (Yazdchi 1999).

The earthquake used was HELLA 2000 $M_0 = 6.5$ in Iceland and the recorded motion of the earthquake were used unmodified and assumed correct. For normal structures it can be assumed that excavated soil is replaced by the structural mass at the site so little changes should be in SSI frequency. This is however not valid for very stiff and heavy structures and special analysis must be conducted to take into account the change of the SSI frequency (Wilson 1995).

Modeling of squat wall and the SSI

Near-field FEM model

A finite element model is used to represent the near-field, figure 1. All elements are treated as solids with three degrees of freedom activated (translations in the nodal x, y, and z direction). Dynamic analysis is carried out using ANSYS. All these necessary elements are available in ANSYS. Solid65 capable of cracking in tension and crushing in compression is used to represent the lightly reinforced C25 concrete. Solid45 is used to represent the soil (Moaveni 2003) linear-plastic properties are used to define the soil.

To model the contact between the wall and the ground the area between them were made Targe170 to define the surface for the contact element. Conta174 is used to represent contact and sliding between elements, the contact element overlays the solid boundaries between the wall and the soil and interacts with them through their surface element when it penetrates one of the target segment elements. The properties of this element allow for simulations of the connections between the foundation and the support, the coefficient of friction being 0.6 for the gravel isolation layer. Contact opening stiffness was chosen as no tension was allowed to form in the contact element. Also a dead weight of $111,8 \text{ kN/m}^2$ is added on the top of the wall to represent roof load. The values used for the elements in these calculations can be seen in Table 1. Equation 1 shows how the shear modulus G and Lamé's constant λ , assuming elastic and isotropic behavior of the elements is obtained.

Two models are built, squat wall from one story height concrete building. Other model is on 0.5m gravel bed as are in common in various parts of Iceland and the other model is fixed on rock to reference. Figure 2

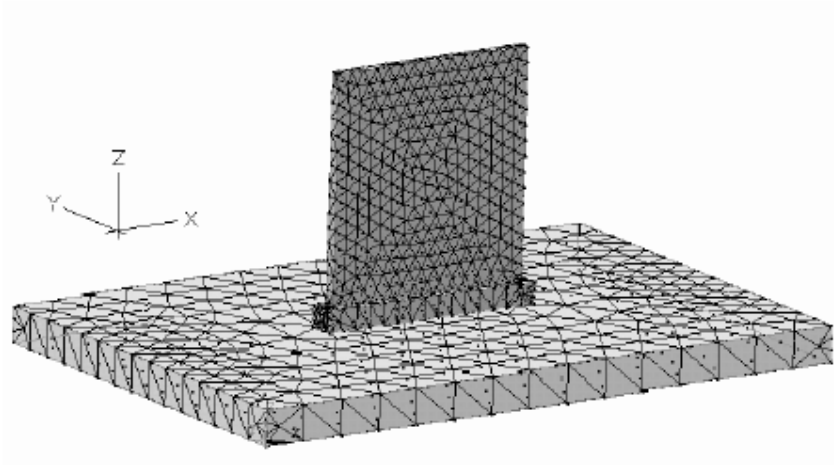


Figure 1: A figure of the near-field SSI system considered in this study.

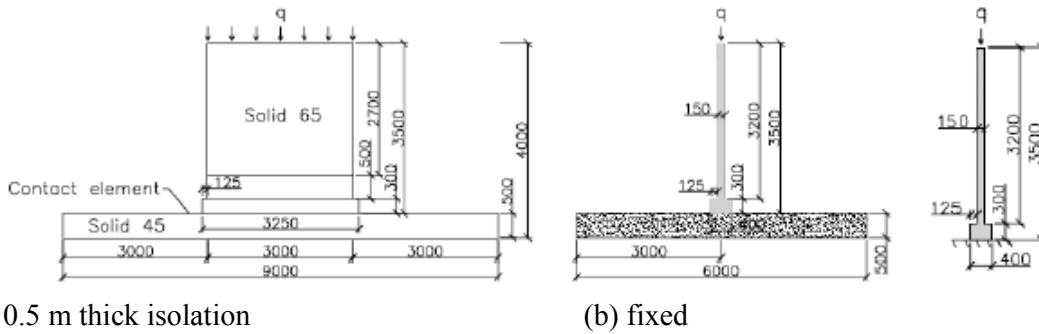


Figure 2: Dimensions for the models being analyzed.

Element	$E(N/m^2)$	$G(N/m^2)$	$\rho(kg/m^3)$	ν^*	$\lambda(N/m^2)$	$v_s(m/s)$	$v_p(m/s)$
Concrete	$25 \cdot 10^9$	N/A^{**}	2380	0.15	N/A	N/A	N/A
Rebar Steel	$210 \cdot 10^9$	$81 \cdot 10^9$	7800	0.30	N/A	N/A	N/A
Mean Gravel	$70 \cdot 10^6$	$30 \cdot 10^6$	1631	0.15	$13,04 \cdot 10^6$	136,60	212,88

Table 1: Setup of a squat wall foundation on support. * Poisson's ratio not to be confused with $v_{p,s}$ which is the wave propagation velocity of the material. **Program controlled, non-linear properties of the concrete, uncracked shear coefficient 0,15 uniaxial tensile strength 4,0MPa and uniaxial compressive strength 30,0MPa.

$$G = \frac{E}{2(1 + \nu)} \quad \lambda = \frac{E \cdot \nu}{(1 + \nu)(1 - 2\nu)} \quad (1)$$

Far-field BEM viscous boundaries

To numerically solve the far-field infinity, viscous boundaries had to be placed at the truncation of the near- and far-field. Although in most cases isolation and foundation devices behave nonlinearly it is common to use linear analysis (Spyrakos 2009). To calculate its effects on the truncated boundaries, the far-field is simplified as an isotropic homogeneous elastic medium. A plane wave propagating in the x-direction is examined (Livaoglu 2007) for this case as shown in figure 3. The equation for equilibrium in one dimension is:

$$\varphi \frac{\delta^2 u}{\delta t^2} - \frac{\delta \sigma_x}{\delta x} = 0, \quad (2)$$

Where φ , u and σ_x are mass density, displacement and stress in the x direction. The change in stress to mass and displacements (and acceleration is second derivative of displacement and φ is density) can be related as:

$$\varphi \frac{\delta u}{\delta t^2} = \frac{\delta \sigma_{xx}}{\delta x} + \frac{\delta \sigma_{xy}}{\delta y} + \frac{\delta \sigma_{xz}}{\delta z} \quad (3)$$

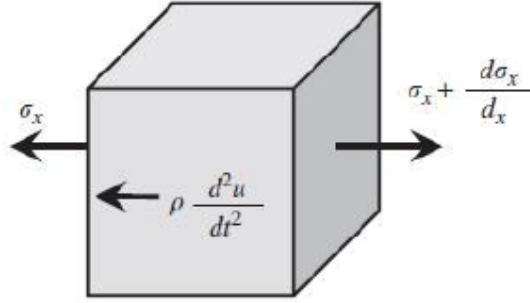


Figure 3: Forces acting on a unit cube

Substituting the appropriate units and with some calculations the wave equation can be obtained. Equation 4 and the velocity of shear wave and pressure wave respectively, equation 6.

$$\varphi \frac{\delta^2 u}{\delta t^2} = (\lambda + 2G) \frac{\delta \Delta}{\delta x_i} + G \nabla^2 \quad (4)$$

Where

$$\Delta = \frac{\delta u_x}{\delta x} + \frac{\delta u_y}{\delta y} + \frac{\delta u_z}{\delta z} \quad \nabla^2 = \frac{\delta^2 u}{\delta x^2} + \frac{\delta^2 u}{\delta y^2} + \frac{\delta^2 u}{\delta z^2} \quad (5)$$

and finally the wave velocity through the far-field medium is:

$$v_p = \sqrt{\frac{\lambda + 2G}{\varphi}} \quad v_s = \sqrt{\frac{G}{\varphi}} \quad (6)$$

λ is the Lamé constant for the material in question and G the shear modulus. The speed of pressure and shear waves travelling through a homogenous and isotropic medium has been obtained, the viscous boundaries are determined by the area of the elements for each damper and the ϕ of the material, which is the force acting at the truncated boundaries is equal to the velocity times the damping constant.

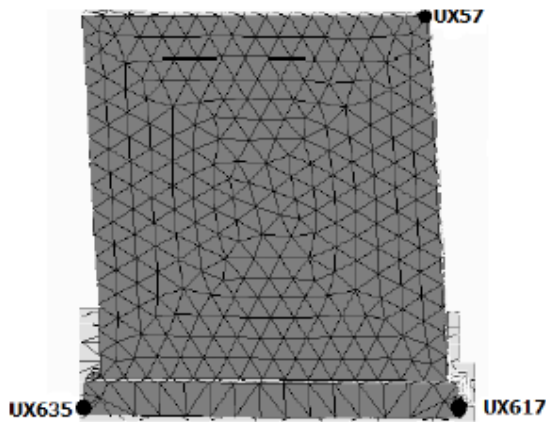
$$N = A\sigma \quad N + C\dot{u} = 0 \quad (7)$$

Where the damping matrix can be written as:

$$C = \begin{bmatrix} A\phi v_p & 0 & 0 \\ 0 & A\phi v_s & 0 \\ 0 & 0 & A\phi v_s \end{bmatrix} \quad (8)$$

Matrix27 is used to represent this damping matrix. It is an arbitrary element without a specified geometry but its response can be specified by stiffness, damping or mass coefficients. The matrix's translational degrees of freedom are activated for one node while the other node has no function and are fixed, thus negating all forces at the truncated boundaries according to equations 7 and 8.

Analysis results



Three nodes are chosen to monitor the nodal translation over time, one at the top and other at the bottom, to see the translation in the x-direction, and the last one at the bottom to monitor rocking or translation in the z-direction. The points can be seen in figure 4. When the wall is fixed the bottom displacement equals the earthquake ground motion, no rocking can occur and only the displacements at the top node are monitored. The near-field calculations are considered as an undamped case and the effects of the far-field considered as a damped case.

Figure 4: Points where translation and rocking is monitored.

Translation in x-direction

The ground motion can be seen in figure 5. It can also be seen that the difference in displacement between the wall's top node and ground is almost nonexistent, the wall is very stiff, and the lag between the bottom displacement and top displacement is very little.

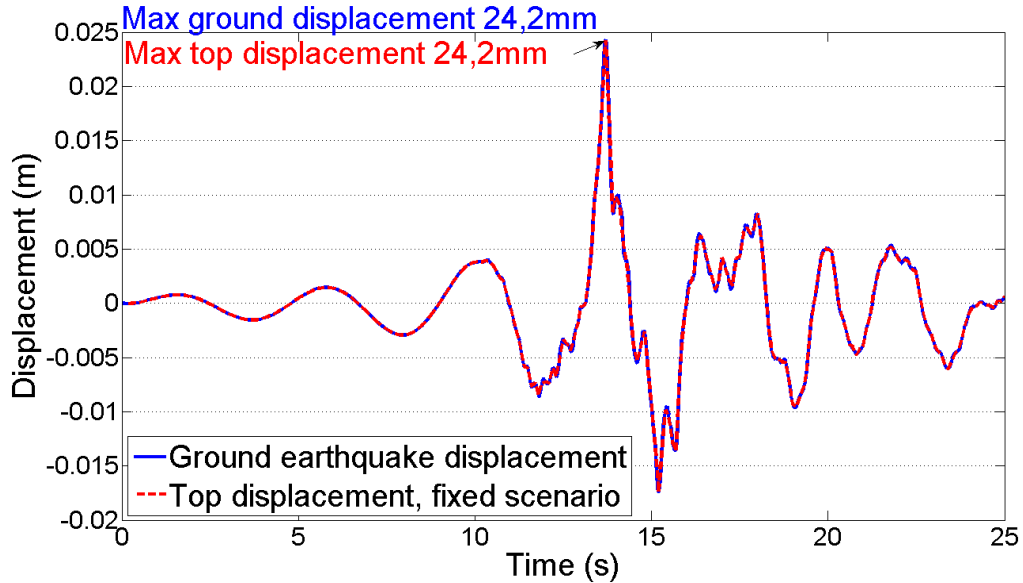


Figure 5: Fixed wall earthquake ground displacement and translation at top node UX57.

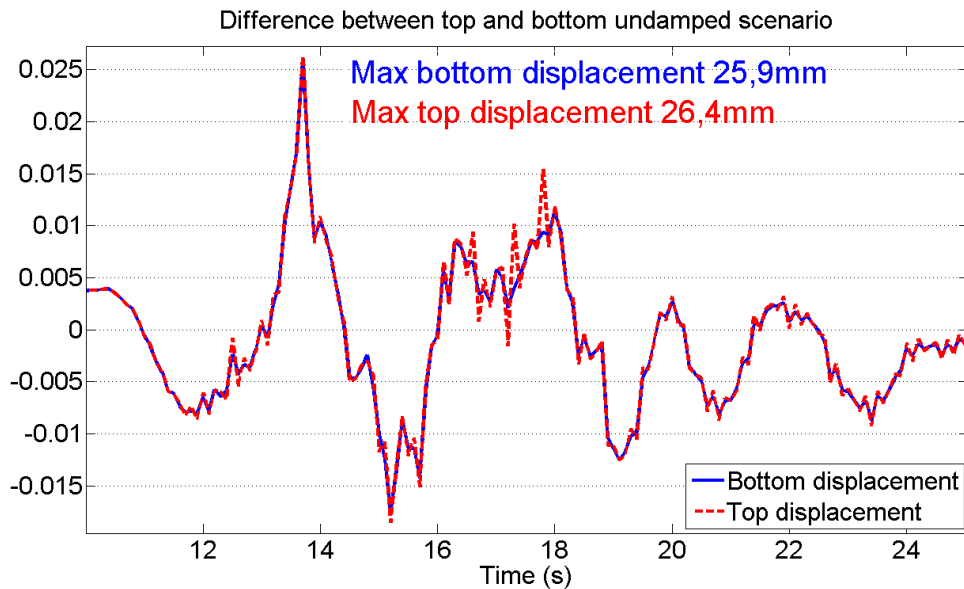


Figure 6: Displacements of bottom and top node for the wall on 0,5m thick isolation layer in an undamped scenario.

Figure 6 shows the difference in motion between the bottom node and top node for the wall on 0,5m isolation layer in an undamped scenario. It shows that sliding occurs between the isolation layer and the wall, the difference between base movement and top movement is also greater due to rocking.

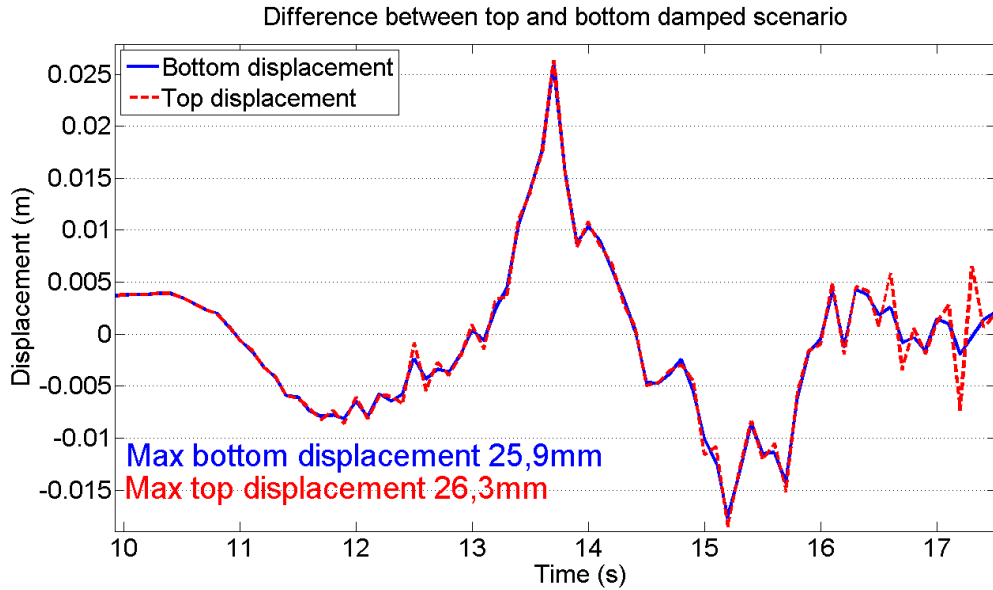


Figure 7: Displacements of bottom and top node for the wall on 0; 5m thick isolation layer in a damped scenario.

Figure 7 shows the same scenario as figure 6 but now taking into account the far field effects. For absolute displacement values it does not have any significant effects, compared to undamped scenario.

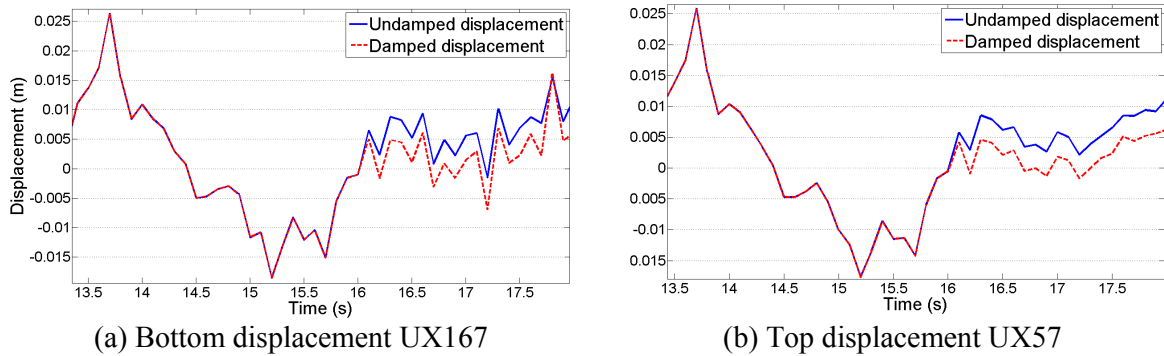


Figure 8: Nodal displacements for a wall on a 0,5 m thick isolation layer

Figure 8 compares the difference in between damped and undamped scenario, leading to the impact the movements are the same, after the impulse the results change. The equilibrium of the near-field is not compromised while the displacements are small but after the impulse the displacements of the damped scenario are reduced. For cases with multi impulse earthquake the effects of far-field could prove more important than for this case where the records used can be classified as single impulse earthquake.

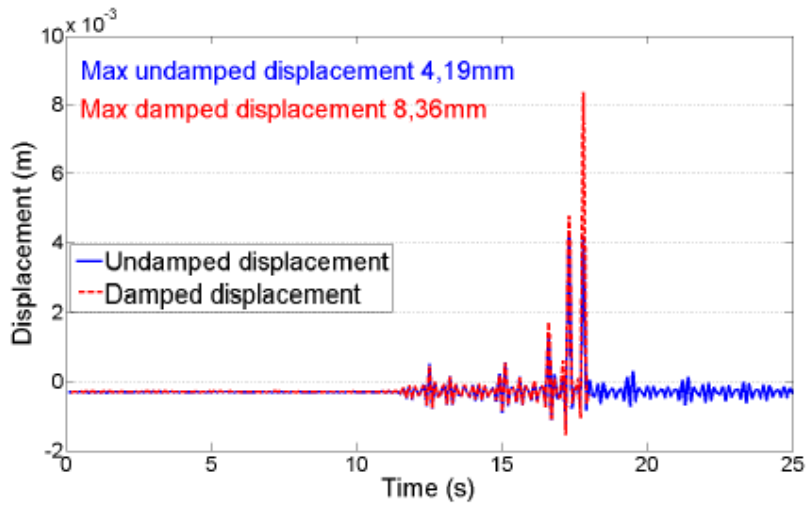


Figure 9: Nodal displacement for rocking in the z-direction UX635

As figure 9 shows, the rocking effects are in place and benefit the energy dissipation of the wall, and displacements also increase when the far-field is taken into account. The stiffness of the wall decreases and the seismic behavior of the wall changes profoundly from the fixed case scenario.

Stress distribution

Scenario	Absolute shear stresses (MPa)	Max compression stresses (MPa)	Max tensile stresses (MPa)
Fixes case	0.169	-0.751	0.297
Undamped	0.090	-0.379	0.017
Damped	0.082	-0.426	N/A

Table 2: List of maximum stresses for shear in the x-direction. Compression and tension in the z-direction during the earthquake, for clarification compression has negative values and tension positive values.

Table 2 shows that the stress decreases when the wall is allowed to rock and translate, the shear stresses are around 50% less for walls founded on a thin gravel isolation layer than when rigidly fixed. Due to rocking compression forces are also in the same region 45-50% lower and tension stresses forces almost non-existent because of the rocking.

Conclusions

These results are in accordance with what has been previously stated: the effects of rocking of the wall change its behavior profoundly, displacements increased while the stresses diminished. This shows that design cases where fixidity is assumed, as is the common practice, the reinforcement ratio is overdesigned. This has also been shown in the South Iceland earthquakes in the years 2000 and 2008 ($M_w=6.5$ and $M_w=6.3$), as poorly reinforced structures on gravel beds escaped with less damage than would have been expected; the earthquake forces having lesser impact on these structures because of the translation and rocking the support allowed.

References

- Apostolou, M., G. Gazetas, and E. Garin, 2007. Seismic response of slender rigid structures with foundation uplifting. *Soil Dynamics and Earthquake Engineering*, 27(7):642-654, 7.
- Dutta, S.C., K. Bhattacharya, and R. Roy, 2004. Response of low-rise buildings under seismic ground excitation incorporating soil-structure interaction. *Soil Dynamics and Earthquake Engineering*, 24(12):893-914, 12.
- Livaoglu, R., and A. Dogangun, 2007. Effect of foundation embedment on seismic behavior of elevated tanks considering fluid-structure-soil interaction. *Soil Dynamics and Earthquake Engineering*, 27(9):855-863, 9.
- Moaveni, S., 2003. *Finite Element Analysis Theory and Application with ANSYS*. Pearson Education, Inc., New Jersey.
- Spyrakos, C.C., I. A. Koutromanos, and Ch. A. Maniatakis, 2009. Seismic response of base isolated buildings including soil-structure interaction. *Soil Dynamics and Earthquake Engineering*, 29(4):658-668, 4.
- Wilson, E. L., 1995. *Three Dimensional Static and Dynamic Analysis of Structures*. Computers and Structures, Inc. Berkeley, California 94704 USA.
- Yazdchi, M., N. Khalili, and S. Valliappan, 1999. Dynamic soil-structure interaction analysis via coupled finite-element-boundary-element method. *Soil Dynamics and Earthquake Engineering*, 18(7):499-517, 10.
- Zhang, J., and Y. Tang, 2009. Dimensional analysis of structures with translating and rocking foundations under near-fault ground motions. *Soil Dynamics and Earthquake Engineering*, 29(10):1330-1346, 10.